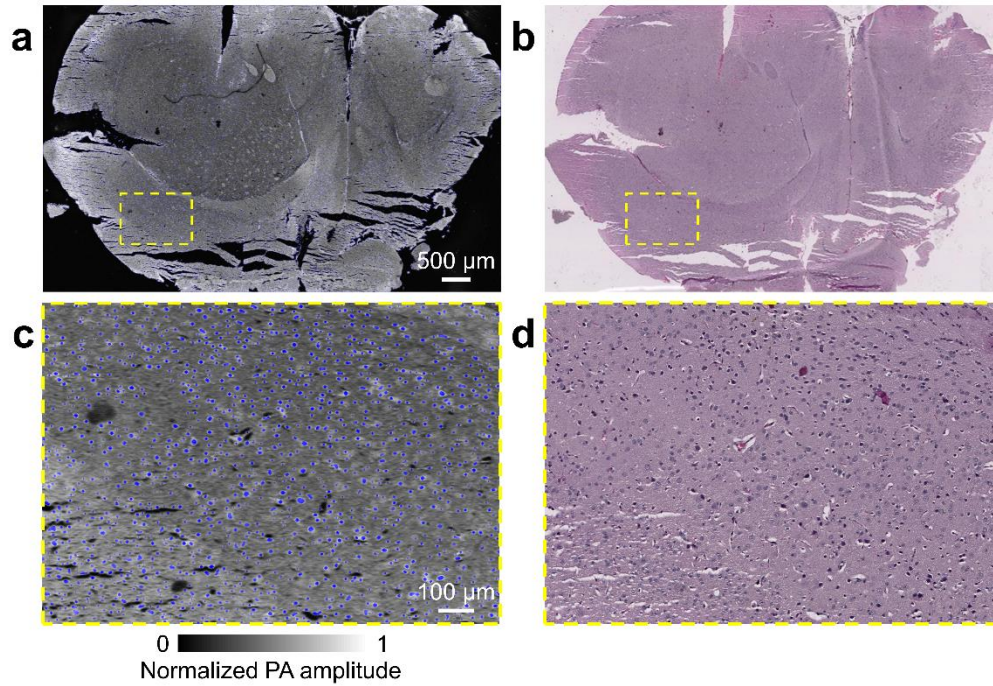
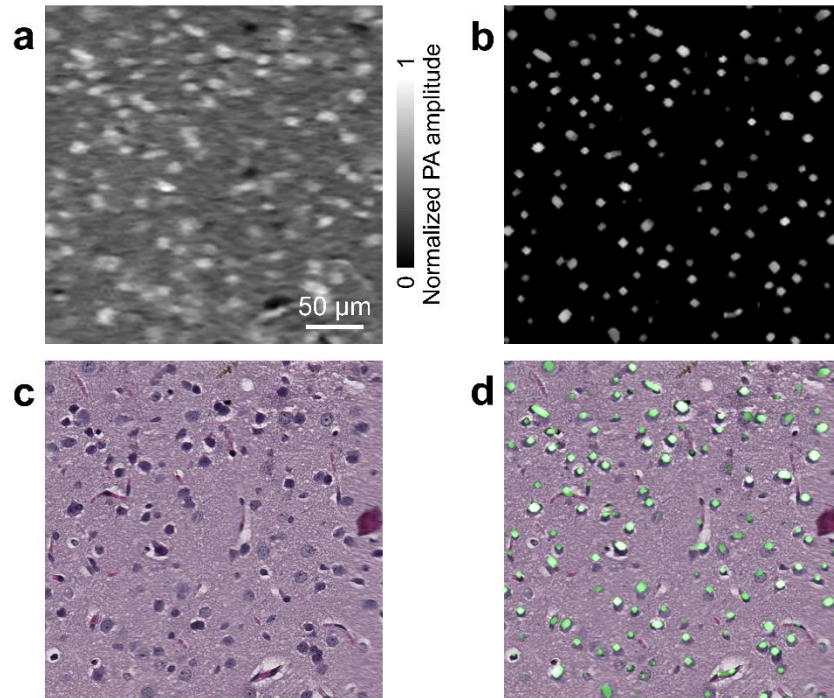


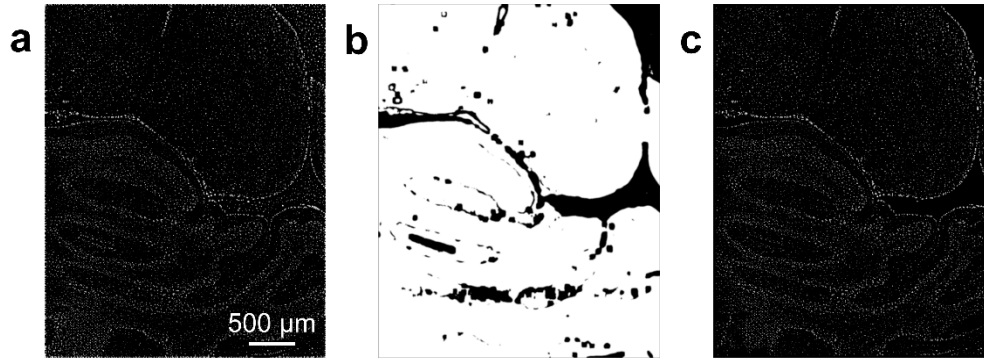
**Supplementary Figure 1.** Resolution of mPAM. **(a)** Zemax design of the optical objective for focusing UV light into water. AL, aspheric lens; CCL, concave lens; CVL, convex lens. **(b)** By imaging a sharp edge and fitting the data to the error function, the system's point spread function (PSF), which is a product of two orthogonal line-spread functions, is obtained. The lateral resolution of mPAM, defined by the full-width at half maximum of the PSF, is 0.91  $\mu\text{m}$ .



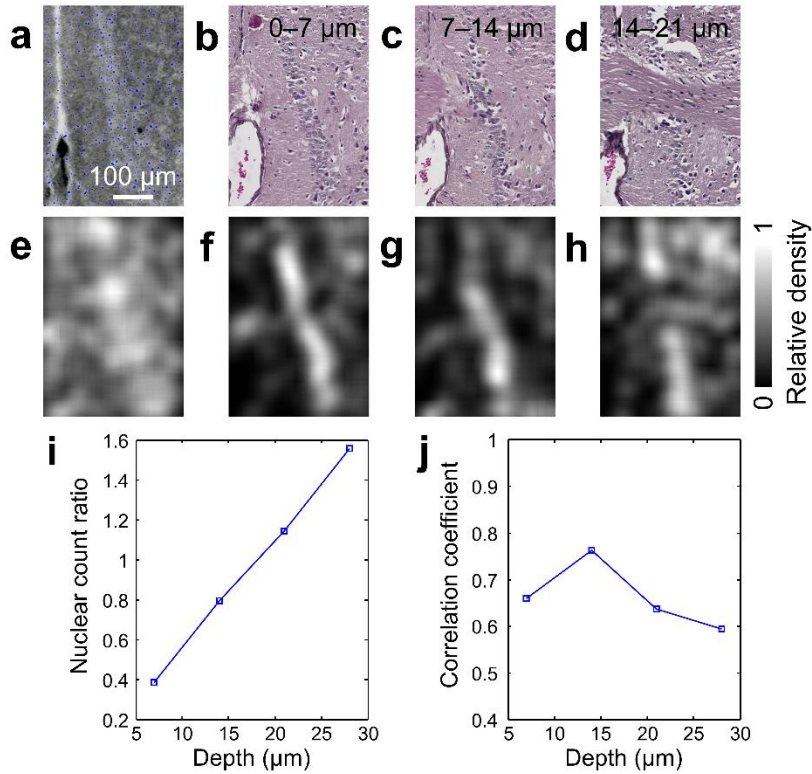
**Supplementary Figure 2.** Imaging of a paraffin section of a mouse brain. **(a)** Label-free mPAM image, where the cell nuclei are enhanced by a Hessian filter and marked in blue. **(b)** Optical microscopy image acquired after H&E staining. **(c),(d)** Close-up images of **(a)** and **(b)**, respectively, corresponding to the yellow dashed regions in **(a)** and **(b)**. The nuclei are clearly resolved by mPAM.



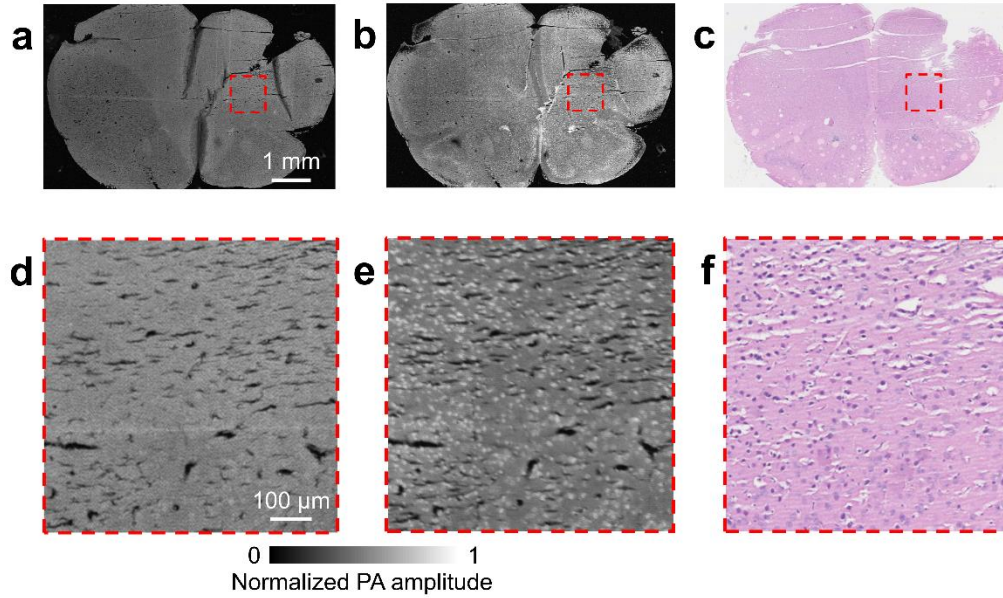
**Supplementary Figure 3.** Comparison between mPAM and H&E images of a paraffin mouse brain section. **(a)** Label-free mPAM image. **(b)** Nuclei extracted from **(a)** by a Hessian filter. **(c)** Optical microscopy image acquired after H&E staining. **(d)** Superimposed image of **(b)** and **(c)**, with **(b)** pseudo-colored in green.



**Supplementary Figure 4.** Extracting nuclei from label-free mPAM images of a mouse brain embedded in a paraffin block. **(a)** Fig. 2c processed by a Hessian filter. **(b)** Nuclear mask calculated from Fig. 2c, which separates tissue (bright) from paraffin (dark). **(c)** Nuclear image obtained by masking **(a)** with **(b)**.

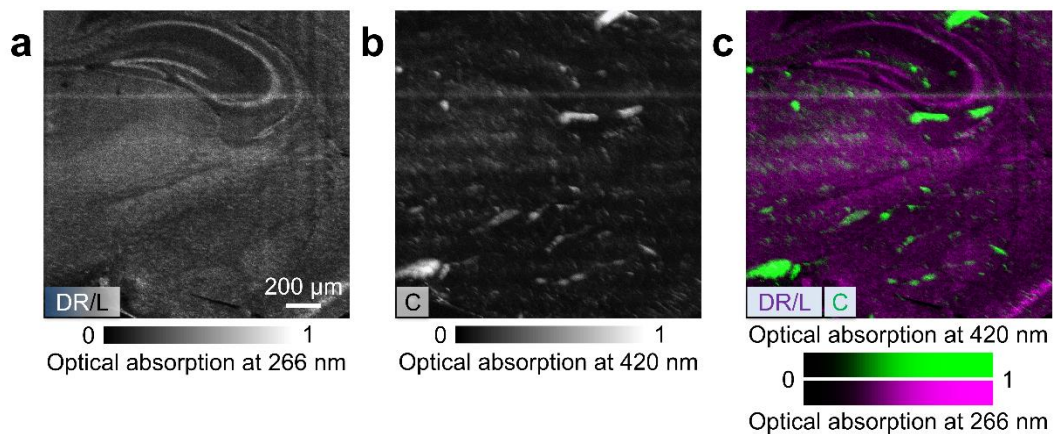


**Supplementary Figure 5.** Imaging depth of mPAM in a tissue block. (a) mPAM image of a paraffin block surface, with nuclei marked in blue. (b)–(d) H&E images of paraffin sections sliced from the block surface in sequence, each with a 7 μm thickness. (e)–(h) Nuclear density maps of (a)–(d), respectively. (i) The ratio of the nuclear count in the H&E images within the given depth range to that in the mPAM image. (j) The correlation coefficient between the nuclear density map of the H&E images within the given depth range and that of the mPAM image.

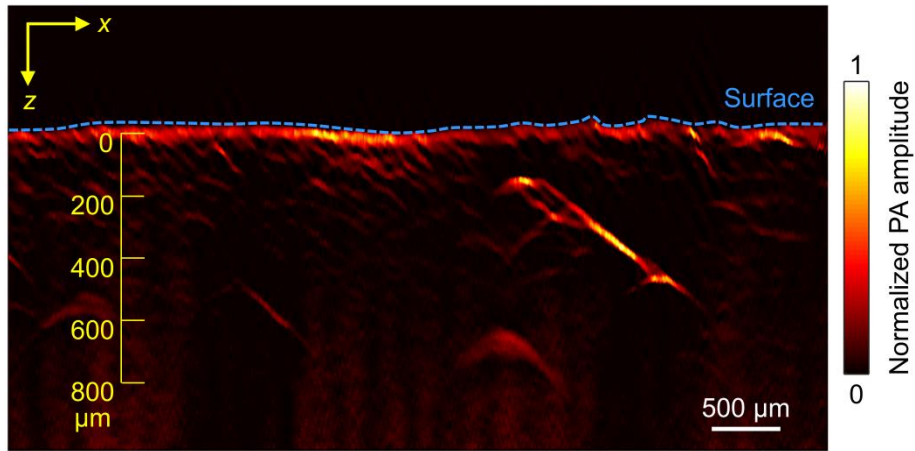


**Supplementary Figure 6.** Imaging of paraffin-embedded and deparaffinized sections of a mouse brain. **(a)** Label-free mPAM image of the paraffin section. **(b)** Label-free mPAM image of the deparaffinized section. **(c)** Optical microscopy image of the adjacent section after H&E staining. **(d)–(f)** Close-up images of **(a)–(c)**, respectively, corresponding to the red dashed regions in **(a)–(c)**. The mPAM image of the deparaffinized section shows cell nuclei clearly without resorting to image processing by Hessian filter.





**Supplementary Figure 7.** Imaging of an agarose-embedded mouse brain section by mPAM with dual wavelengths. **(a)** Label-free mPAM image with 266 nm laser illumination, which mostly shows DNA/RNA (DR) and lipid (L) contrasts. **(b)** Label-free mPAM image with 420 nm laser illumination, which shows cytochrome (C) contrast. **(c)** Overlay image of **(a)** and **(b)**, where pseudo colors are used to illustrate the optical absorption color contrast of the biomolecules.



**Supplementary Figure 8.** Representative xz projected 1 mm thick mouse brain image acquired over  $6.0 \times 0.1 \text{ mm}^2$ . The blue dashed line outlines the surface of the mouse brain. With 420 nm light illumination, the deepest cytochrome contrast based structures are  $\sim 800 \mu\text{m}$  in depth measured from the mouse brain surface.